Supplementary information for

Projecting changes in rainfall-induced landslide susceptibility across China under climate change

Jinqi Wang [1, 2], Hao Fang [2,3,4], Kai Liu [1, 2*], Yi Yue [2], Ming Wang [1, 2], Bohao Li [1, 2], Xiaoyi Miao [1, 2]

[1] Joint International Research Laboratory of Catastrophe Simulation and Systemic Risk Governance, Beijing Normal University, Zhuhai 519087, China

[2] School of National Safety and Emergency Management, Beijing Normal University, Beijing 100875, China.

[3] Zhejiang Institute of Geosciences, Hangzhou 310007, China

[4] Qiantang Institute of Geosciences, Hangzhou 310007, China

*Corresponding author: Kai Liu (liukai@bnu.edu.cn)

Contents of this file

Supplementary Table

Supplementary Table S1: Comparison of simulated precipitation and observed precipitation (The root mean square error (RMSE) for different models)

ID	Model	RMSE	Mean RMSE (574.60)
1	IPSL-CM6A-LR	561.81	
2	BCC-CSM2-MR	567.90	
3	MPI-ESM1-2-HR	568.80	
4	INM-CM5-0	568.86	
5	ACCESS-CM2	569.07	
6	NESM3	569.17	
7	CanESM5	569.96	
8	UKESM1-0-LL	570.11	
9	CNRM-ESM2-1	570.14	
10	KIOST-ESM	570.22	RMSE ≤ Mean RMSE
11	EC-Earth3	570.34	
12	HadGEM3-GC31-LL	570.76	
13	EC-Earth3-Veg-LR	570.87	
14	CNRM-CM6-1	571.33	
15	MIROC-ES2L	571.73	
16	FGOALS-g3	571.80	
17	GISS-E2-1-G	572.02	
18	NorESM2-LM	572.61	
19	ACCESS-ESM1-5	573.04	
20	INM-CM4-8	573.18	
21	MRI-ESM2-0	575.14	
22	IITM-ESM	576.75	
23	MPI-ESM1-2-LR	577.33	
24	GFDL-ESM4	577.53	
25	NorESM2-MM	577.96	
26	MIROC6	578.38	RMSE ≤ Mean RMSE
27	CESM2	579.36	
28	CMCC-ESM2	580.93	
29	TaiESM1	581.35	
30	CMCC-CM2-SR5	596.12	
31	KACE-1-0-G	607.04	

Notes:

(1) RMSE is calculated using the formula provided above, which compares simulated and observed annual precipitation totals for each model.

(2) Mean RMSE is 574.60, representing the average RMSE across all models.

(3) Models with an RMSE ≤ mean RMSE are considered to have better simulated accuracy relative to the overall dataset.

Formula:

The RMSE is calculated as follows:

$$RMSE = \sqrt{\frac{1}{n}\sum_{i=1}^{n}(O_i - P_i)^2}$$

Where:

(1)n is the number of grid cells (pixels) in the raster,

(2)O_i is the observed precipitation at the $i-th$ grid cell,

(3)P_i is the predicted precipitation at the $i-th$ grid cell.

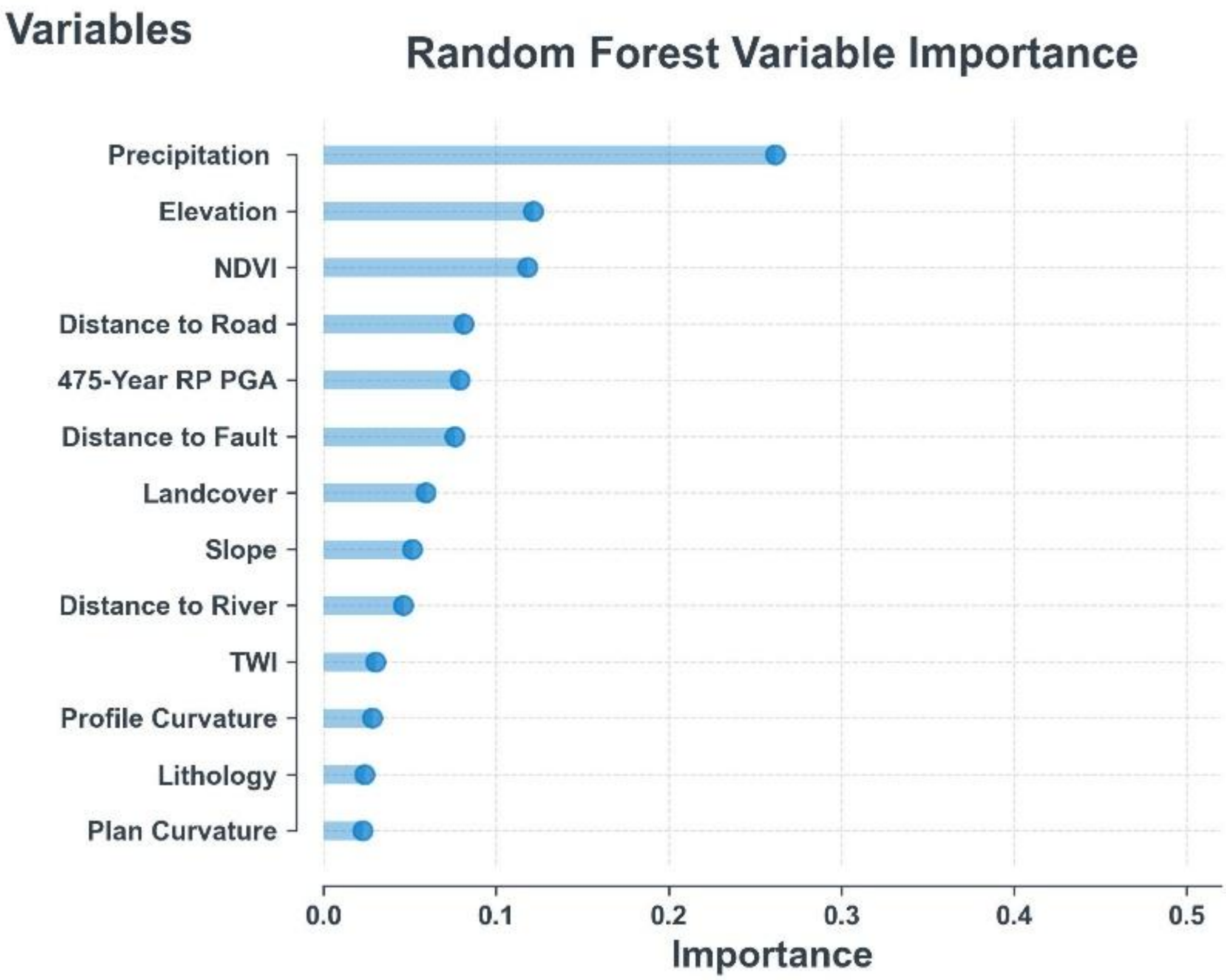

Supplementary Fig. S1: Relative importance of landslide conditioning factors as determined by the random forest (RF) model.

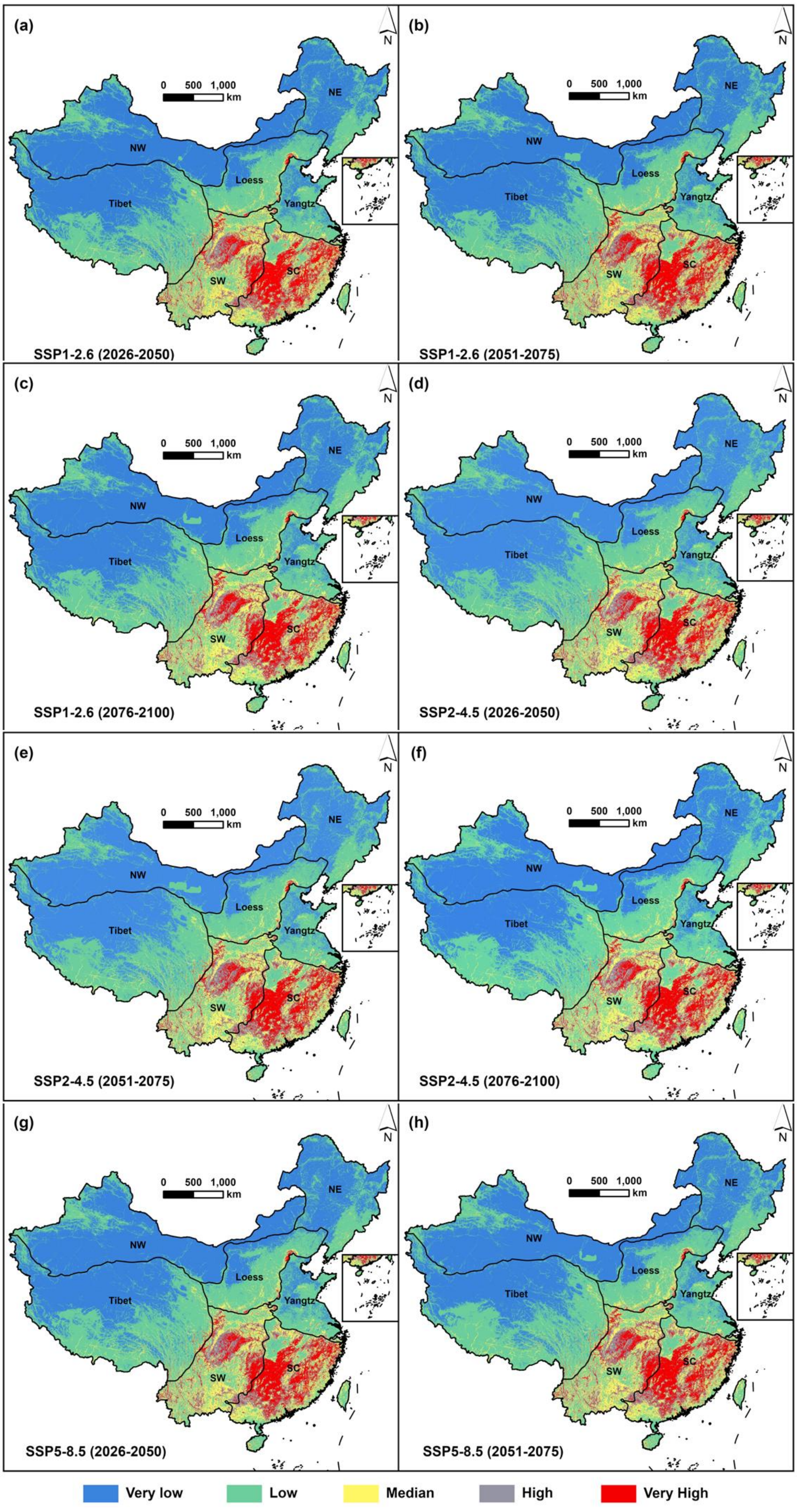

Supplementary Fig. S2: Spatial pattern of landslide susceptibility in China during future periods: near-term future (2026–2050), mid-term future (2051–2075), and long-term future (2076–2100) under SSP1-2.6, SSP2-4.5, and SSP5-8.5.

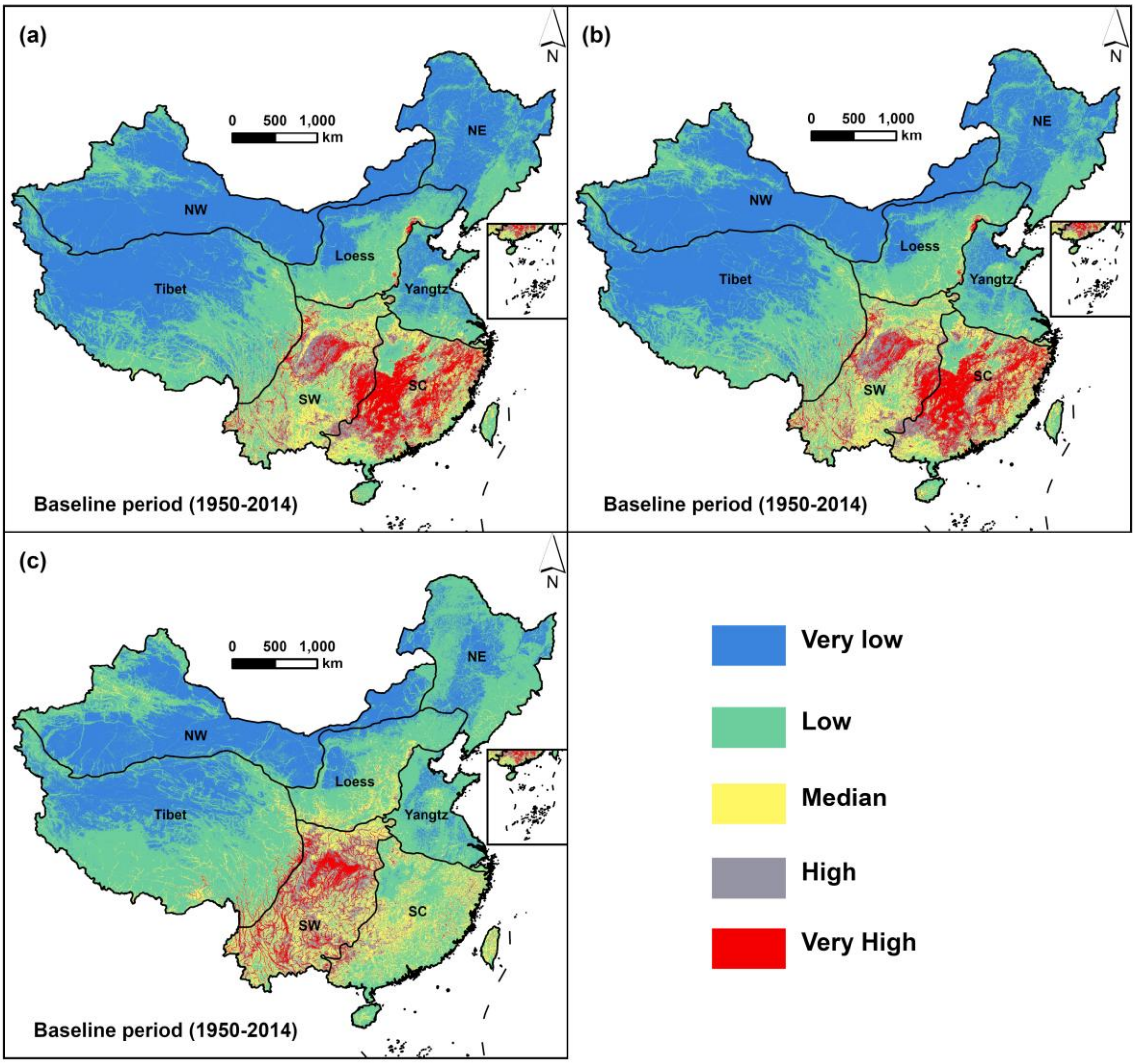

Supplementary Fig. S3: Landslide susceptibility maps illustrating the effect of thematic accuracy (i.e., completeness of small landslide records) on model results. (a) Baseline map constructed from the complete inventory (AUC = 0.97); (b) Map after removing 50% of the small landslides from the inventory (AUC = 0.97); (c) Map after completely excluding small landslides from the inventory (AUC = 0.96).

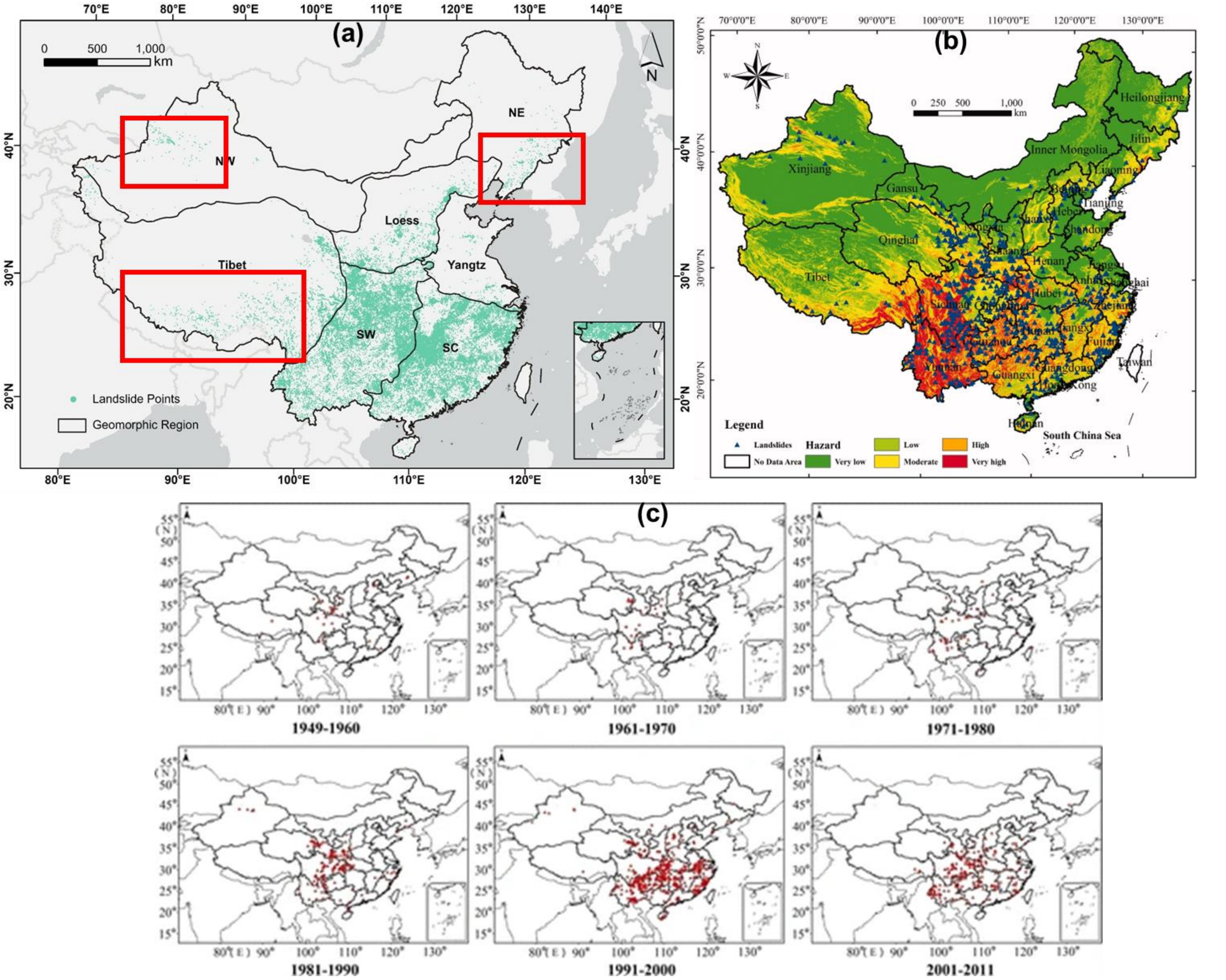

Supplementary Fig. S4: Comparison of landslide inventories. (a) Landslide points used in this study; (b) National-scale landslide inventory from Liu and Miao (2018); (c) National-scale landslide inventory from Liu et al. (2013).

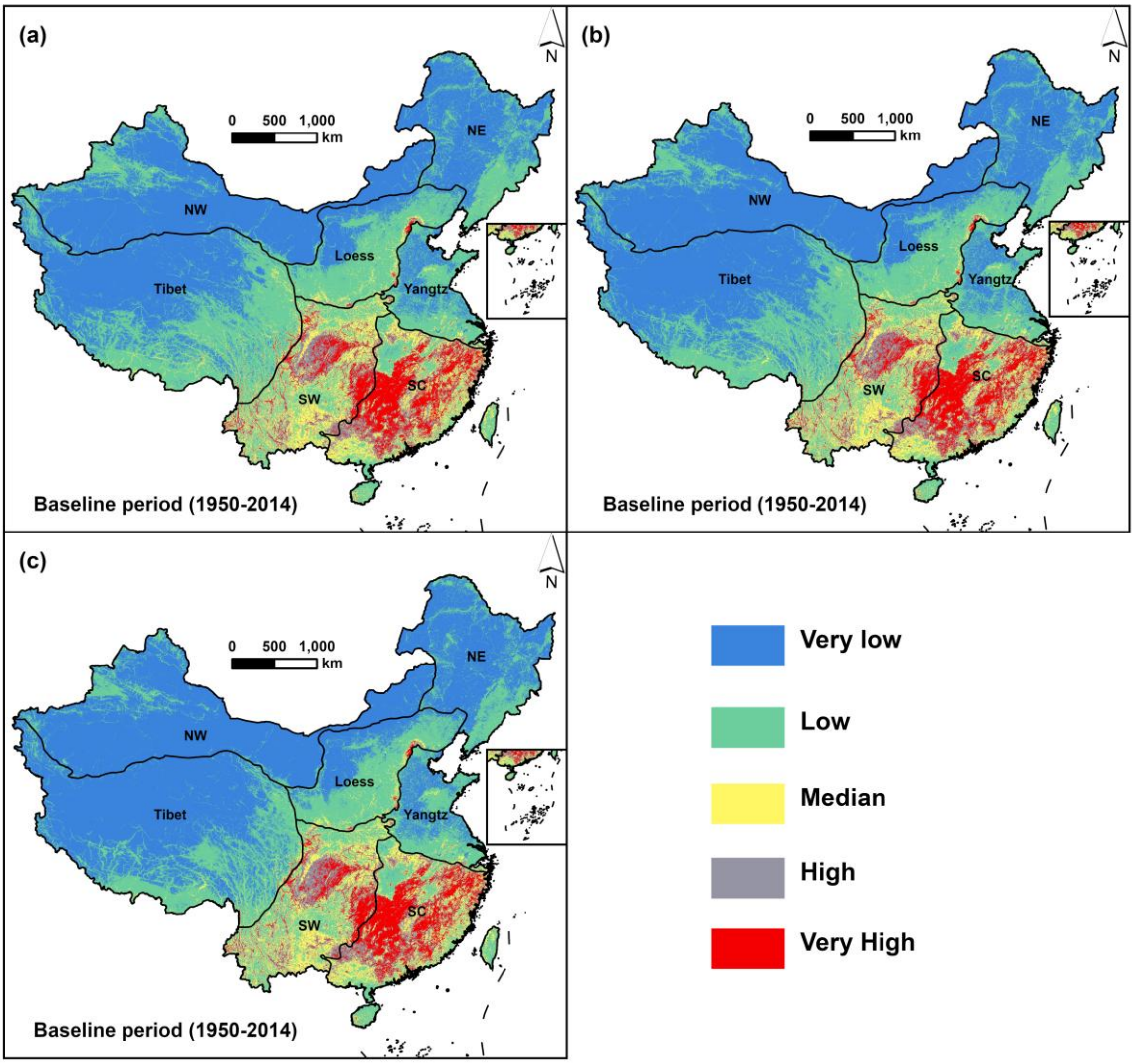

Supplementary Fig. S5: Landslide susceptibility maps generated from inventories with different levels of completeness in Northwest (NW), Northeast (NE), and Tibet regions (AUC = 0.97). (a) Baseline map using the complete inventory; (b) Map after randomly removing 50% of landslide points in the target regions (AUC = 0.97); (c) Map after randomly removing 75% of landslide points in the target regions (AUC = 0.97).